MISSOURI S&T

Missouri University of Science and Technology

Scholars' Mine

Physics Faculty Research & Creative Works

Physics

Temperature and Supersaturation Dependent Nucleation Rates of Heterogeneous Water by Molecular Cluster Model Calculation

Chen K. Lutrus

Donald E. Hagen
Missouri University of Science and Technology, hagen@mst.edu

Sung-Ho Suck Salk

Recommended Citation

C. K. Lutrus et al., "Temperature and Supersaturation Dependent Nucleation Rates of Heterogeneous Water by Molecular Cluster Model Calculation," *Journal of Chemical Physics*, vol. 99, no. 12, pp. 9962-9971, American Institute of Physics (AIP), Aug 1993.
The definitive version is available at https://doi.org/10.1063/1.465395

Temperature and supersaturation dependent nucleation rates of heterogeneous water by molecular cluster model calculation

Chen K. Lutrus and Donald E. Hagen
Cloud and Aerosol Science Laboratory, University of Missouri, Rolla, Missouri 65401

Sung Ho Salk
Department of Physics, Pohang Institute of Science and Technology, Korea

A statistical mechanical method to evaluate the energy of formation of water clusters attached to a foreign particle surface is described, with the binding energy being evaluated on a molecular level, using semiempirical modified neglect of diatomic overlap (MNDO) theory. The model is applied to water nucleation on a silicon oxide surface. The binding energy contribution, which represents the energy of formation at $T=0$ K, is found to slightly (but not negligibly in the thermal sense) increase with the number of hydrogen bonds between the water cluster and the condensation nucleus whose surface is made of silicon oxide. An analytic expression is developed to fit the binding energy contribution as a function of cluster size. At lower temperatures, a linear relationship is found between the log of the nucleation rate and reciprocal temperature for fixed saturation ratio. However, at higher temperatures, this relationship deviates from linearity. The deviation is sufficient to suggest the existence of a critical temperature for which the nucleation rate reaches a maximum. Furthermore, another kind of critical temperature is found, which corresponds to a minimum cluster critical size (at fixed saturation ratio). These are found to almost coincide for the cases of heterogeneous and homogeneous nucleation.

I. INTRODUCTION

A study of the interaction between the silicon oxide surface and water may have important implications to semiconductor fabrication technology. Furthermore, despite a longstanding need for basic understanding of gas-to-particle conversion, present knowledge of the role of heterogeneous nucleation in the initiation of gas-to-particle conversion is severely deficient. As an example, cloud[1-5] and aerosol[6-8] formation in the atmosphere are initiated by heterogeneous nucleation and condensation processes on foreign particles. Cloud droplets and aerosols thus formed are subject to further growth by coalescence. Foreign particles enhance nucleation with varying degrees of efficiency. An understanding of this heterogeneous nucleation requires basic (microphysical and chemical) knowledge,[9-16] e.g., about the interactions between vapor phase molecules and the surface of the foreign particle. Due to its intrinsic nature, such a fundamental study requires a microphysical (molecular level) treatment.

A successful first principles treatment of water cluster properties and their interactions with foreign surfaces is necessary for a microphysical model of water nucleation. A computationally efficient semiempirical effective Hamiltonian method[17-19] for treating molecular clusters was recently developed and applied to pure water for homogeneous nucleation studies.[17,20,21] This treatment led to reliable intermolecular binding energies and electronic properties for hydrogen-bonded water clusters in agreement with *ab initio* calculations,[22] while other semiempirical methods failed.[23] Physical properties such as ionization potentials, dipole moments, and normal mode vibrational frequencies were found to be in good agreement with experiments[24-27] and theory.[22-28] In the present study, this methodology is extended to the case of heterogeneous water nucleation.

The contents of the present work are divided into three categories: (1) a statistical mechanical description for the energies of formation for heterogeneous clusters; (2) the use of a molecular level effective Hamiltonian approach to compute the electronic binding energy involved in the statistical mechanical treatment; and (3) a report on the computed results for both energies of formation and nucleation rates.

II. STATISTICAL MECHANICAL DESCRIPTION OF THE ENERGY OF FORMATION AND NUCLEATION RATE FOR HETEROGENEOUS CLUSTERS

Earlier, we presented a classical electrothermodynamic description for the free energy of formation of hydrated ion clusters.[29] Here, we would like to study the energy of formation and nucleation rate for heterogeneous clusters at finite temperatures based on both quantum and statistical-mechanical treatments. In the multistate-kinetics approach to nucleation,[30] the energy of formation at critical size is needed for the evaluation of nucleation rate. Such a model had been developed earlier for the case of homogeneous nucleation[17,20,21] and had been used to calculate the energy of formation and nucleation rate for homogeneous water clusters. Here the model is adapted to the case of heterogeneous nucleation.

We consider a system composed of a molecular gas and suspended foreign particles. Gas phase molecules (water monomers) W_1 and the foreign particles (silicon oxide, which act as condensation nuclei) X are subject to interaction to form heterogeneous clusters of size i. The multistate-kinetics processes of interest are $X + W_1 \rightleftharpoons XW_1$

and $XW_{i-1} + W_1 \rightleftharpoons XW_i$ with $i = 2, 3, 4, \ldots$. For simplicity, the distinguishability of configurations for the clusters is ignored.

The law of mass action for the process above is written

$$N_i / (N_{i-1} N_1) = q_i / (q_{i-1} q_1). \tag{2.1}$$

Here, N_i is the total number of the heterogeneous cluster XW_i, and q_i is its partition function. N_1 is the total number of the vapor phase monomers W_1, and q_1 is its partition function. Applying successive substitution, expression (2.1) leads to

$$N_i = (N_X / q_X)(N_1 / q_1)^i q_i, \tag{2.2}$$

where N_X stands for the total number of foreign particles X, and q_X is its partition function.

Unless the temperature is exceedingly high, coupling between the electronic and nuclear (translational, vibrational, and rotational) motions is negligible. Thus, we write

$$q_i = \xi_i \xi_i^e, \tag{2.3}$$

where ξ_i^e is the ground state electronic partition function. In the limit of weak coupling between nuclear motions, ξ_i can be approximated by the product of translational (ξ^t), rotational (ξ^r), and vibrational (ξ^v) partition functions

$$\xi_i = \xi_i^t \xi_i^r \xi_i^v. \tag{2.4}$$

Denoting E_X, E_1, and E_i as the electronic ground state energies of the foreign particle X, monomer W_1, and heterogeneous cluster XW_i, respectively, for the electronic part of the partition function, the substitution of Eq. (2.3) into Eq. (2.2) above yields

$$N_i = N_X N_1^i [\xi_i / (\xi_X \xi_1^i)] \exp(-\Delta E_i / kT), \tag{2.5}$$

where ΔE_i is the total binding energy of cluster i corresponding to $T = 0$ K,

$$\Delta E_i = E_i - (E_X + iE_1). \tag{2.6}$$

We now rewrite the expression (2.5)

$$N_i = N_X N_1 \exp\{-[\Delta E_i - kT(\ln \xi_i - i \ln \xi_1 - \ln \xi_X)$$
$$- (i-1)kT \ln N_1] / kT\}. \tag{2.7}$$

Denoting the number concentration of cluster i by $n_i = N_i / V$, with V being the volume, and writing

$$\ln(N_1 / V) = \ln(N_1 / N_1^0) + \ln(N_1^0 / V) = \ln S + \ln n_1^0,$$

with n_1^0 denoting the number concentration of the monomer at equilibrium (at given temperature) and S the saturation ratio, we obtain from Eq. (2.7) above

$$n_i = n_X n_1 \exp\{-[\Delta E_i - kT(\ln \xi_i' - i \ln \xi_1' - \ln \xi_X')$$
$$- (i-1)kT(\ln S + \ln n_1^0)] / kT\}, \tag{2.8}$$

with $\xi' = \xi / V$ and $n = N / V$.

We now cast Eq. (2.8) into a form

$$n_i = n_X n_1 \exp(-\Delta \Phi_i / kT), \tag{2.9}$$

where $\Delta \Phi_i$ is defined to be the energy of formation of the heterogeneous clusters

$$\Delta \Phi_i = \Delta E_i - kT(\ln \xi_i' - i \ln \xi_1' - \ln \xi_X') - (i-1)kT \ln n_1^0$$
$$- (i-1)kT \ln S, \tag{2.10}$$

or simply,

$$\Delta \Phi_i = \Delta E_i - kT(\ln \xi_i' - i \ln \xi_1' - \ln \xi_X')$$
$$- (i-1)kT \ln(P/kT), \tag{2.11}$$

where P is the water monomer partial pressure.

It is now clear from Eq. (2.10) or Eq. (2.11) that at 0 K, the formation energy of cluster i is simply reduced to the electronic energy ΔE_i. The second term in Eq. (2.10) or Eq. (2.11) represents the change of free energy from the vapor phase of the monomer to the cluster of size i, due solely to a change in the contribution of nuclear (translational, rotational, and internal vibrational) motion at a finite temperature $T \neq 0$. The last term in Eq. (2.11) plays the role of enhancing order for the stability of clusters at finite temperatures. The intensive parameter S or P acts as an "external field" to stabilize the cluster.

The ultimate goal of nucleation theory is to evaluate the nucleation (droplet formation) rate at which gas-to-particle phase transition occurs. The nucleation rate J is given by[30]

$$J = \alpha \exp(-\Delta \Phi_{i*} / kT). \tag{2.12}$$

Here, i^* is the critical cluster size for which $\Delta \Phi$ reaches a maximum; α is the prefactor

$$\alpha = \beta \sigma F n_1 Z, \tag{2.13}$$

where β is the sticking coefficient; σ is the critical size cluster surface area; $F = n_1 \sqrt{8kT / \pi m}$ is the monomer flux; and n_1 is the concentration of the monomer. Here, z is the Zeldovitch factor[30]

$$Z = \left(\frac{-(\partial^2 \Delta \Phi_i / \partial i^2)_{i=i*}}{2\pi kT} \right)^{1/2}. \tag{2.14}$$

In the next section, we discuss the energy of formation and nucleation rates in more detail in order to cast them into calculable forms.

III. COMPUTATIONAL TREATMENT OF THE ENERGY OF FORMATION AND THE NUCLEATION RATES FOR HETEROGENEOUS WATER CLUSTERS

Here, we discuss computation of the formation energy (binding energy) ΔE_i at 0 K and other terms that appear in Eq. (2.10). First, for the formation energy of the heterogeneous water cluster at 0 K, we express the total binding energy of cluster i as

$$\Delta E_i = \Delta E_{X-W} + \Delta E_{W-W}, \tag{3.1}$$

where

$$\Delta E_{X-W} = E_{XW_i} - (E_X + E_{W_i}), \tag{3.2}$$

and

$$\Delta E_{W-W} = E_{W_i} - iE_{W_1}. \tag{3.3}$$

This is to express the energy ΔE_i in terms of an interaction energy between the (pure) water cluster and the foreign particle in the heterogeneous cluster ΔE_{X-W}, and an energy representing water–water intermolecular interactions in the homogeneous water cluster ΔE_{W-W}.

We use an effective Hamiltonian method[31] modified neglect of diatomic overlap (MNDO) to calculate binding energies for the heterogeneous cluster (E_{XW_i}), the homogeneous water cluster (E_{W_i}) the foreign particle (E_X), and the water monomer (E_{W_1}). Earlier we reparametrized the method to suit systems involving water.[18] The reparametrization involves the parameters for hydrogen and oxygen atoms only. Using this version of the computer code, hereafter called HMNDO (hydrogen bond corrected version of MNDO), we had predicted the energy, ionization potential, and other physical properties of the water cluster very well.[18] Furthermore, we had included the electronic energy in the calculation of the energy of formation and the nucleation rates for homogeneous water clusters and found good agreement with experimental results.[17,20,21] However, up to that point, we were only able to treat systems involving pure water. Here, the HMNDO parametrization has been incorporated into an improved version of MNDO, called AM1,[32] which is well suited to treat systems containing silicon. Details concerning our modifications are given in the Appendix.

In our earlier work on homogeneous water clusters,[21] we found that a function of the form

$$B_i = B_\infty (1 - i^{-\theta}) \tag{3.4a}$$

could be used to fit the binding energy per bond as a function of cluster size. Here we use this same functional form to represent the water–water interaction term ΔE_{W-W}. The adjustable parameters take on the values $B_\infty = -0.58$ eV (-13.4 kcal/mol) and $\theta = 0.5$. Now assuming that the structure of the water cluster is open (no rings), i.e., the number of bonds in the cluster is equal to the number of monomers minus one. With this, the energy between water molecules in the homogeneous water cluster becomes

$$\Delta E_{W-W} = (i-1) B_\infty (1 - i^{-\theta}). \tag{3.4b}$$

The determination of nucleation rates requires a focus of attention at the cluster critical size, where the energy of formation $\Delta \Phi_i$ reaches a maximum. Since the water cluster critical size is assumed to be small compared to the condensation nucleus, we treat the heterogeneous water–silicon oxide cluster as a system consisting of a water cluster and a silicon oxide surface. In Fig. 1, we display a 3D perspective of a particular water cluster (five water molecules) on a silicon (111) oxide surface. The circles with letter o represent oxygen atoms, circles with H represent hydrogen, circles with S represent silicon, and the small unmarked circles represent siligen, respectively. Elsewhere[33-35] we have shown the validity of using a limited size silicon cluster to represent a real silicon surface. Siligens,[35] artificial atoms, are used to saturate the dangling bonds, which would otherwise be occupied in the bulk. Oxygens are placed 0.6 Å above the surface at bridge (be-
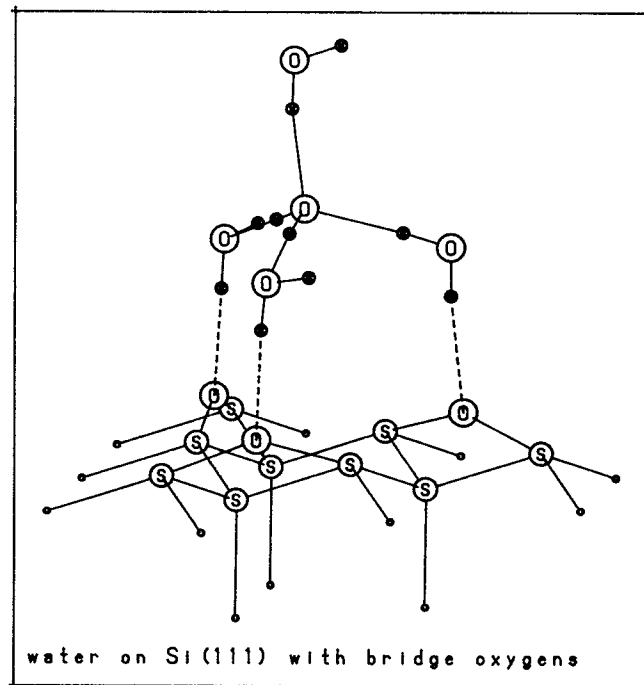

water on Si (111) with bridge oxygens

FIG. 1. A three-dimensional perspective of a particular water cluster on a Si (111) surface.

tween two nearest top-layer silicons) sites, to which the water cluster makes hydrogen bonds (indicated by dashed lines) as the bridge sites are known to be stable configurations.[34,36] In this model, the silicon surface with the siligens, and the oxygens on the bridges represent the foreign particle X, the silicon oxide. We examined several clusters where we maintained the silicon oxide fixed and varied the number of water molecules. We also varied the number of bonds between the water cluster and the surface (the number of dashed lines in Fig. 1). Using the modified AM1-HMNDO version of MNDO, we calculated the energies of the water clusters, the silicon oxide (surface), and the combined systems (the heterogeneous clusters). The binding energies between the water cluster and the silicon oxide surface were calculated following Eq. (3.2). The results are shown in Fig. 2. They showed a slight increase with the number of water–surface bonds. The octagons denote clusters with one water–surface bond, the triangles are for two bonds, and the squares are for three bonds. At $i=0$, the energy should be zero. At $i=\infty$, it should converge to a certain value, since it should not change when a molecule is added to a large cluster. The analytic function of cluster size i,

$$\Delta E_{X-W} = a[1 - (i+1)^{-b}] \tag{3.5}$$

with $a = -4.56$ eV (-105.16 kcal/mol), and $b = 0.5$, is found to fit the results very well and also satisfies the conditions at $i=0$ and infinity. Nishijima et al.,[37] using vibrational electron energy loss spectroscopy on the Si(111)(7 ×7)–H₂O system, estimated the O–H bond energy to be 4.2 eV. Their estimation was based on the Birge–Sponer
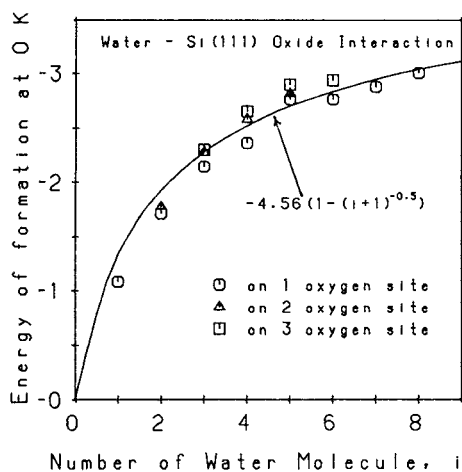
FIG. 2. Electronic binding energy between water clusters and a silicon oxide surface as a function of number of water molecules i.

extrapolation.[38] Thus, our prediction of an asymptotic value of 4.56 eV agrees reasonably well with the experimental value.

Dynamic effects associated with translational, rotational, and vibrational motions, which are depicted in the second term of Eq. (2.10) will now be discussed. Since the nucleating water cluster is attached to the surface, we assume that the nucleus is in a stationary condition compared to the fast moving water molecule in the vapor phase and so is the product heterogeneous cluster. With this assumption, the translational and rotational partition functions of both the heterogeneous cluster XW_i and the foreign particle X are removed from the second term of Eq. (2.10). The translational and rotational partition functions for the water monomer are computed from[30]

$$\xi_1^t = V(2\pi m k t/h^2)^{3/2} \tag{3.6}$$

and

$$\xi_1^r = (\pi I_x I_y I_z)^{1/2} (8\pi^2 kT/h^2)^{3/2}/\eta, \tag{3.7}$$

respectively. Here, m is the water molecule mass; h is the Planck's constant; I_x, I_y, and I_z are the components of principal moments of inertia; and η is the symmetry number; it is 2 for a water molecule.

Assuming that the intramolecular vibrational frequencies of the clusters are relatively unchanged compared to those of the water molecule and likewise for the silicon oxide surface, we write the vibrational contribution of the second term in Eq. (2.10)

$$F^v = -kT(\ln \xi_i^v - i \ln \xi_1^v - \ln \xi_x^v) = F_{W-W}^v + F_{X-W}^v \tag{3.8}$$

with

$$F_{W-W}^v = -kT \ln \xi_{W-W}^v \tag{3.9}$$

and

$$F_{X-W}^v = -kT \ln \xi_{X-W}^v, \tag{3.10}$$

where ξ_{W-W}^v denotes the product of partition functions for the intermolecular vibrational motion between any two water molecules in the pure water cluster, and ξ_{X-W}^v is that for the vibrational motion between the water cluster and the surface. In our earlier treatment of homogeneous water nucleation[17,20,21] we used an analytic function of the form

$$F_{W-W}^v = (i-1)\left[-kT \ln \left(\frac{e^{-A/T}}{1-e^{-B/T}} \right) \right] \tag{3.11}$$

with $A = 1.55 \times 10^3$ K and $B = 2.0$ K, in place of Eq. (3.9). Its use in the energy of formation calculation predicted the nucleation rate of homogeneous water cluster very well. For the current calculation (heterogeneous nucleation), we use the same functional form with the same numerical values for coefficients A and B.

Ibach et al.[30] reported a vibrational frequency of 3420 cm^{-1} in their vibrational study of water on Si (111). It was associated with the hydrogen bond. We use this frequency in our calculation of ξ_{X-W}^v,

$$\xi_{X-W}^v = \prod_{j=1}^{\text{mode}} \left(\frac{e^{-\omega_j/2kT}}{1-e^{-\omega_j/kT}} \right), \tag{3.12}$$

where $\omega_j = 3420$ cm^{-1}. In our current model, we only use one vibrational mode in Eq. (3.12). An increased number of vibrational modes could be included as the cluster size increases. However, we do not currently have any a priori argument to define the correct number of modes for a given cluster size.

The water vapor equilibrium concentration n_1^0, which appears in the third term of Eq. (3.10) is given by

$$n_1^0 = \frac{P^0}{kT}, \tag{3.13}$$

where P^0 is the equilibrium vapor pressure of pure water.[40]

We now rewrite Eq. (2.10) in a calculable form

$$\Delta \Phi_i = a[1-(i+1)^{-b}] + (i-1)B_\infty(1-i^{-\theta})$$
$$+ ikT \ln \left(\frac{\xi_1^t}{V} \right) + ikT \ln \xi_1^r + F_{W-W}^v - kT \ln \xi_{X-W}^v$$
$$- (i-1)kT \ln n_1^0 - (i-1)kT \ln S. \tag{3.14}$$

To calculate the nucleation rate J in Eq. (2.12), we set β the sticking coefficient to unity. The water cluster (critical size) surface area σ is that corresponding to a sphere containing i^* water molecules. This assumption of using a spherical pure water cluster model will affect the magnitude of the nucleation rate only by a multiplication factor. As the predicted nucleation rate is presented in the log scale, the effect of the multiplicative factor will be to shift the entire curve up by some fixed amount. Errors in this factor therefore will not alter the qualitative discussion we are presenting.

The Zeldovitch factor, defined in Eq. (2.14), takes the form

$$Z = \left\{ \frac{ab(b+1)(i+1)^{-b-2} - B_\infty \theta i^{-\theta-1}[1-\theta+(\theta+1)i^{-1}]}{2\pi kT} \right\}^{1/2}$$

(3.15)

for the $\Delta\Phi_i$ shown in Eq. (3.14).

IV. COMPUTATION RESULTS

Using Eqs. (3.1)–(3.15), the energies of formation and nucleation rates are calculated for various conditions and the results are plotted. In Figs. 3, 4, and 5, we show the dimensionless formation energy $\Delta\Phi/kT$ for water–silicon oxide clusters as a function of number of the water molecules i, for various saturation ratios, at fixed temperatures 220, 270, and 320 K, respectively. The maxima (corresponding to critical size) consistently show decreasing magnitude as the saturation ratio increases. For a given temperature, saturation ratio is related linearly with the number concentration of the water monomer. Thus as the concentration increases, it takes less energy to form the clusters. It is also observed that the critical size (indicated by vertical dashed lines) decreases as saturation ratio increases. The critical sizes are listed in Table I. For $S \geqslant 1$, $\Delta\Phi/kT$ vs i exhibits a minimum at very small cluster sizes. This will lead to small stable clusters forming at this size at surface nucleation sites. This same type of energy minimum was observed in a previous study of hydrated ion cluster nucleation.[29] For the ranges of temperature and saturation ratio used here, these energy minima occurred at cluster sizes between 6 and 12.

For the sake of comparison, we plotted the energy of formation for both homogeneous water clusters and heterogeneous water clusters in Fig. 6. We chose the temperature 300 K and saturation ratios 2 and 3. As expected, the homogeneous clusters' critical size and energy are higher than those for the heterogeneous cluster. Both the smaller

critical cluster size and lower energy barrier imply higher nucleation rates for the heterogeneous path to nucleation.

Figure 7 shows the dimensionless energy of formation (total energy) and its contributive energy terms as described in Eq. (2.10) as functions of cluster size. In order to magnify the change of the total energy of formation [marked (f)], we use a smaller plot scale (right-hand scale) for it. The water monomer's translational and rotational motion terms, which are positive (dissociative) contributions to the energy of formation increase linearly with size, and are indicated by (a). The water–water intermolecular vibrational motion term also increases linearly with size, and is indicated by (b). The water–silicon oxide vibrational motion term is indicated by (c). It is a constant as we account for only one bond between the water and the silicon oxide surface (by bond, here we mean the hydrogen bond between the oxygen of the silicon oxide and the hydrogen of the water cluster). The three energy terms just mentioned are positive (dissociative) energy terms. They represent the change of free energy from the water cluster to the monomer vapor phase. There are two negative energy terms that tend to associate molecules to form a cluster. The first is the formation energy at 0 K [electronic energy term (3.1)], indicated by (d). It includes the binding energies of both the water–water and the water–silicon oxide interactions. The electronic energy term or the formation energy at 0 K by itself is not enough to cause the formation of the cluster at finite temperature. Another negative energy term is the water vapor concentration term, indicated by (e). It acts as an "external field" to stabilize the cluster. At small cluster sizes (lower than 12 water molecules), the negative energy terms are dominant, lead-
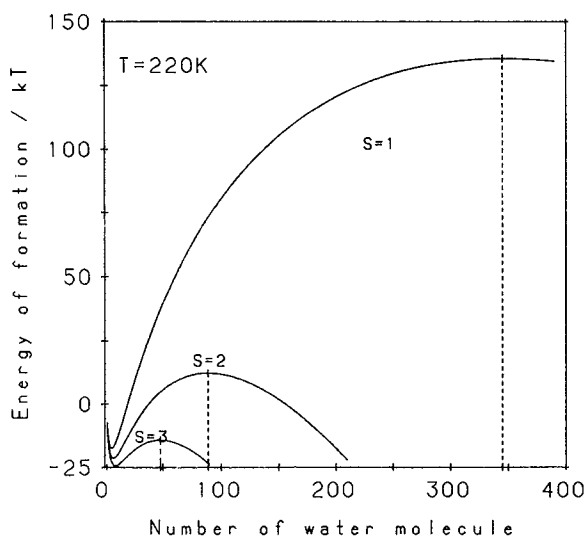

FIG. 3. Dimensionless energy of formation as a function of the number of water molecules i for saturation ratios 1, 2, and 3 at temperature 220 K.
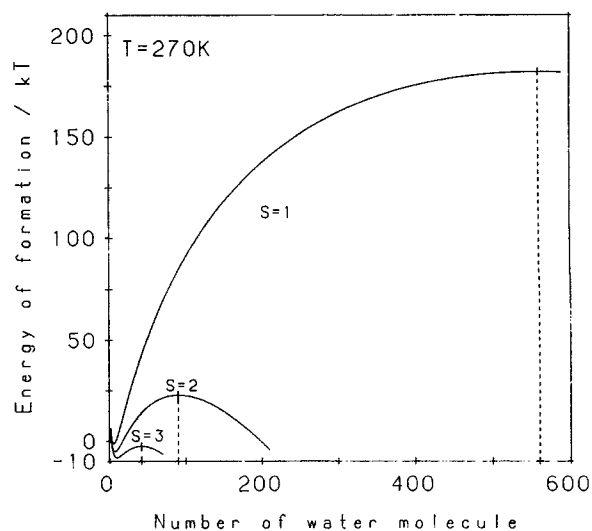

FIG. 4. Dimensionless energy of formation as a function of the number of water molecules i for saturation ratios 1, 2, and 3 at temperature 270 K.
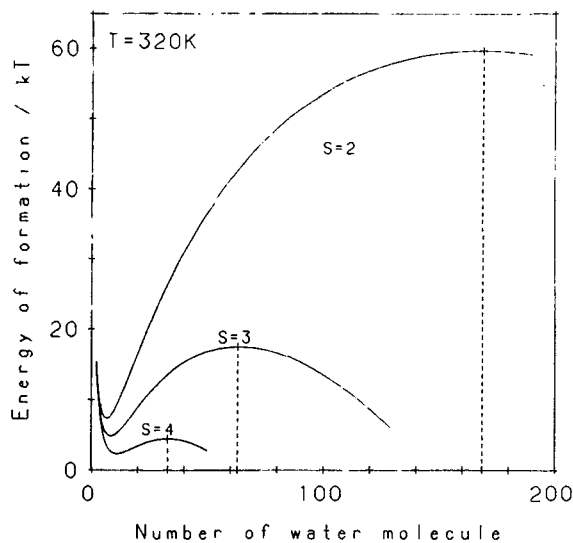
FIG. 5. Dimensionless energy of formation as a function of the number of water molecules i for saturation ratios 2, 3, and 4 at temperature 320 K.
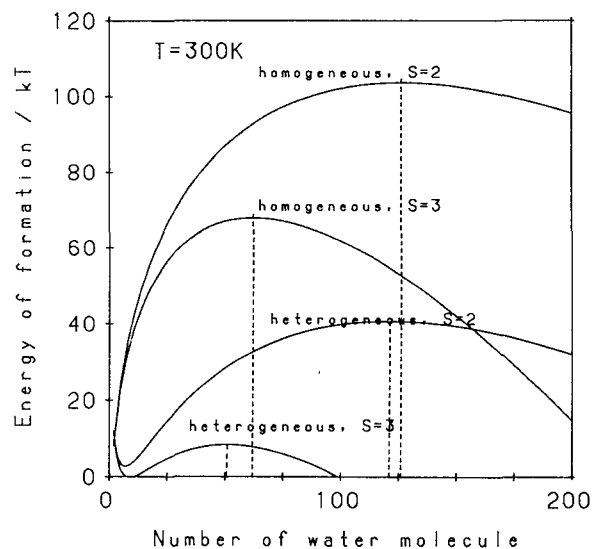

FIG. 6. Dimensionless energy of formation of heterogeneous and homogeneous water clusters as a function of the number of water molecules i for saturation ratios 2 and 3 at temperature 320 K.

ing to the minimum[29] shown in the total energy of formation [curve marked (f)]. As the cluster size increases, the contributions from the dissociative energy terms become dominating, causing the total energy to increase. Eventually, the electronic binding energy and concentration dependent stabilization term take over and cause the total energy to decrease with further increases in size, leading to a peak total energy at a critical cluster size.

In Fig. 8, we display the log of the calculated nucleation rates (J) using Eq. (2.12) vs reciprocal temperature. We find (1) a linear relationship between $\log(J)$ and $1/T$; (2) for a given T, nucleation rate increases as the S increases; and (3) the lines get closer together as the saturation ratio increases, i.e. $(\partial S/\partial T)$ for fixed J increases as T decreases. These same propensities were found earlier[17,20,21] for homogeneous nucleation. As expected, compared to the homogeneous case, heterogeneous nucleation at a fixed rate and supersaturation occurs at a much lower temperature, i.e., for fixed conditions, the heterogeneous nucleation is easier than the homogeneous one.

We now investigate whether the linear $\log(J)$ vs $1/T$ characteristic holds for higher temperatures. At lower temperatures, as temperature increases, the last two terms in Eq. (2.10), which are monomer concentration related and tend to promote cluster binding, dominate over the second term, which is the positive (dissociative) contribution to the formation energy from vibrational, rotational, and

translational motions. This is evidenced by the slope of the line shown in Fig. 8. However, at higher temperatures there are deviations from linearity in the log (J) plot as shown in Fig. 9. This suggests a stronger effect from the dissociative contributions. In fact, for $S=2$ and 3, at temperatures above 230 K, the nucleation rates start to decrease with increasing temperature. This phenomenon can be seen more clearly in Fig. 10. Here we plotted the log (J) against the saturation ratio for different temperatures. There is inversion of the trend as the temperature increases. For a given saturation ratio, e.g., $S=3$, we see that the nucleation rate reaches a maximum ~230 K. Note that in Fig. 9 we did not draw the curves beyond certain temperatures for $S=5$, 7, 10, and 13 because there are no energy of formation barriers with respect to the cluster sizes beyond those temperatures, thus no critical sizes
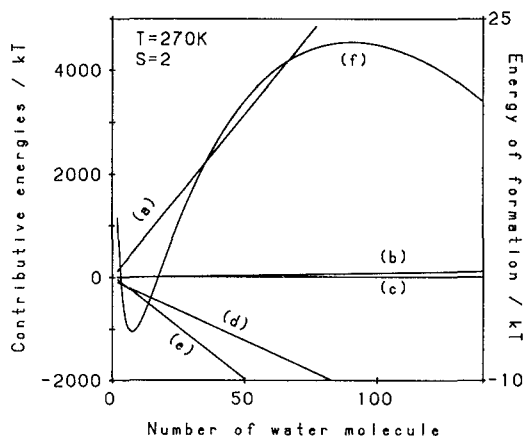
TABLE I. Critical sizes (number of water molecules) of the water–silicon oxide system for some selected temperatures and saturation ratios.

	$T=220$ K	270 K	320 K
$S=1$	345	560	
2	89	90	169
3	48	42	63
4	30	20	33

FIG. 7. Dimensionless contributive energies to the total energy of formation as a function of the number of water molecules i. The right hand scale is particularly for the curve marked (f), the total energy of formation.
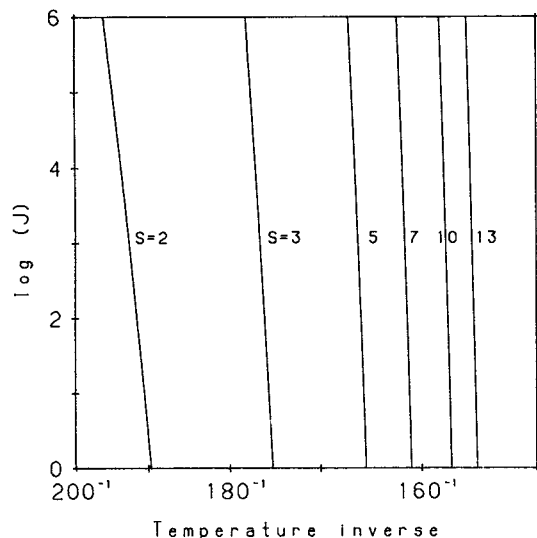
FIG. 8. The log of the nucleation rates of heterogeneous water cluster as a function of temperature inverse for saturation ratios of 2, 3, 5, 7, 10, and 13.
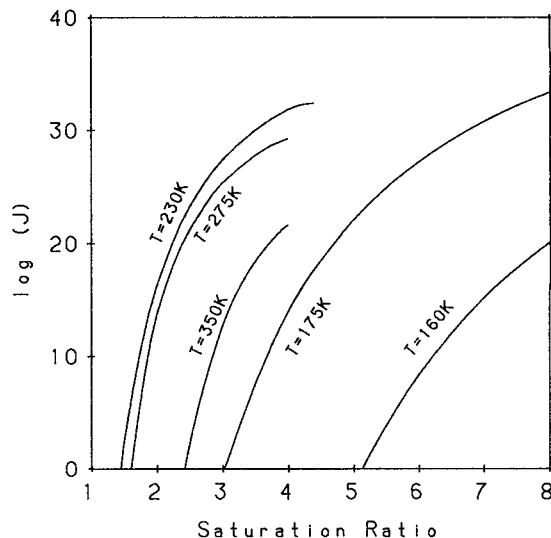
FIG. 10. A log of the nucleation rates of heterogeneous water clusters as a function of saturation ratio for temperatures of 160, 175, 230, 275, and 350 K.

available for us to calculate the nucleation rates. In Fig. 10, we also have some of the curves cut beyond a certain saturation ratio for the same reason.

It is also useful to investigate the behavior of critical size as the temperature is increased for fixed saturation ratio. In Figs. 11, 12, and 13, we plotted the dimensionless energy of formation for saturation ratios of 2, 3, and 4, respectively. In each plot, we included energy of formation curves corresponding to temperatures 220, 270, and 300 K. As listed in Table I, for $S=2$, i^* increases with temperature, i.e., the i^*'s are ordered in the sequence i^* (220 K), i^* (270 K), and i^* (320 K). However, for $S=3$ and 4, the order is changed to i^* (270 K), i^* (220 K), and i^*

(320 K). We also found the same feature for the homogeneous nucleation case. This is shown in Fig. 14 for $S=5$. This suggests that for a given saturation ratio, there is a minimum critical size corresponding to a certain temperature. Using interpolation, we found those temperatures. These are plotted against the saturation ratio in Fig. 15. The line with octagons depicts the heterogeneous nucleation case, and the one with squares depicts the homogeneous case. The second is close to a continuation of the first. Note that in the region of overlap, e.g., at $S=3$, the temperatures corresponding to minimum critical sizes for both heterogeneous and homogeneous nucleation are almost the same. Hence, the water monomer concentrations are about the same. There appears to be almost no effect on
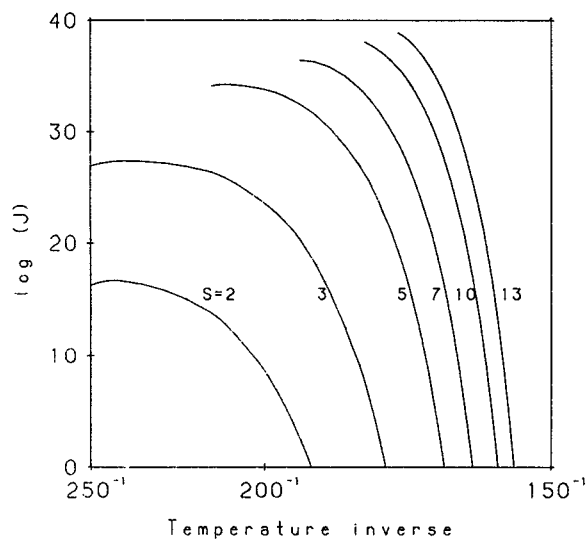
FIG. 9. A log of the nucleation rates of heterogeneous water clusters as a function of temperature inverse for saturation ratios of 2, 3, 5, 7, 10, and 13 with a larger range of temperature and nucleation rate than Fig. 6.
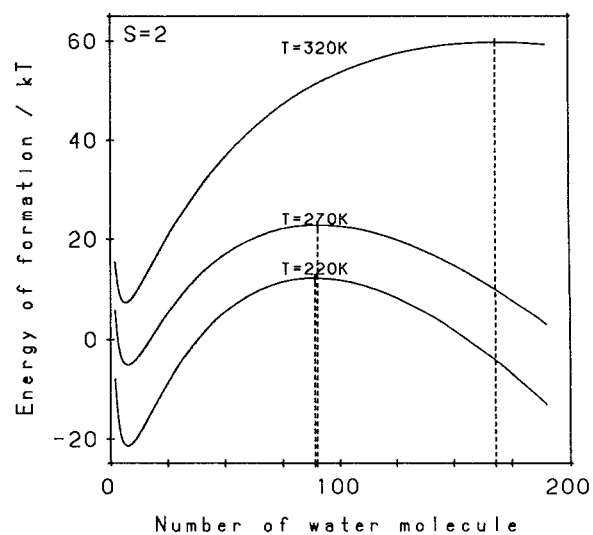
FIG. 11. Dimensionless energy of formation as a function of the number of water molecules i for temperatures of 220, 270, and 320 K at a saturation ratio of 2.
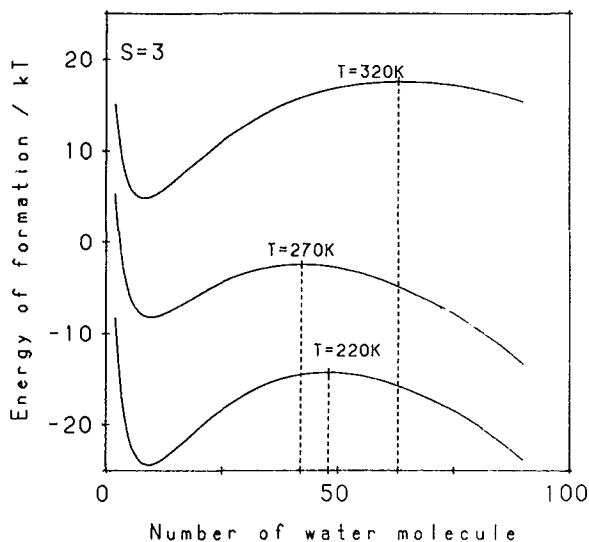
FIG. 12. Dimensionless energy of formation as a function of the number of water molecules i for temperatures of 220, 270, and 320 K at a saturation ratio of 3.

FIG. 14. Dimensionless energy of formation of homogeneous water clusters as a function of the number of water molecules i for temperatures of 220, 270, and 320 K at a saturation ratio of 5.

the temperature (and thus on the concentration) to minimum critical cluster size associated with the existence of the nucleus in the case of heterogeneous nucleation. It would be interesting to see in the future if this feature holds for different nucleus materials. In Fig. 16, we plotted minimum critical sizes (corresponding to the temperatures in Fig. 15) against saturation ratio. Although at fixed saturation ratio (e.g., at $S=3$ and also at 4) they occurred at almost the same temperatures, the magnitudes of the minimum critical sizes between the two cases are quite different, with the heterogeneous case being smaller.
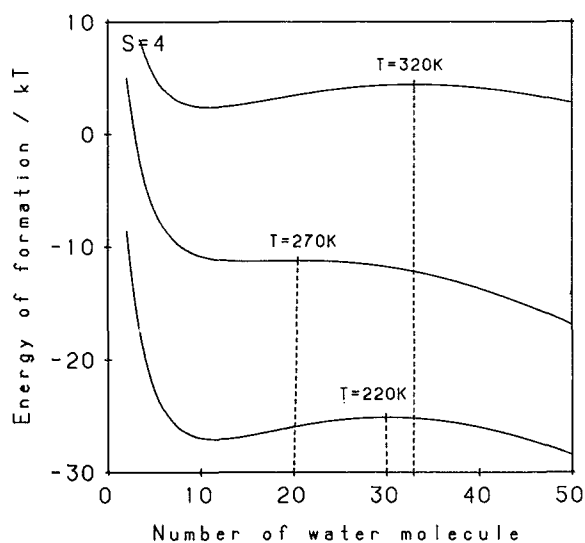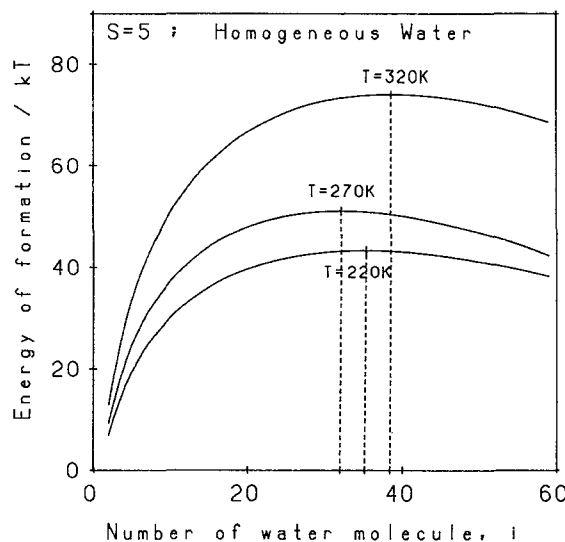
V. CONCLUSION

In this study, a statistical-mechanical treatment was made to evaluate the energy of formation and the nucleation rate for heterogeneous nucleation at finite temperature. The formulation has been cast into a form suitable for microscopic treatment. The interaction and vibrational motions between water molecules has been treated in a manner similar to that used previously for homogeneous water clusters. The electronic binding energies between a water cluster and the silicon oxide surface was found to increase sightly with the number of the bonds between the

FIG. 13. Dimensionless energy of formation as a function of the number of water molecules i for temperatures of 220, 270, and 320 K at a saturation ratio of 4.
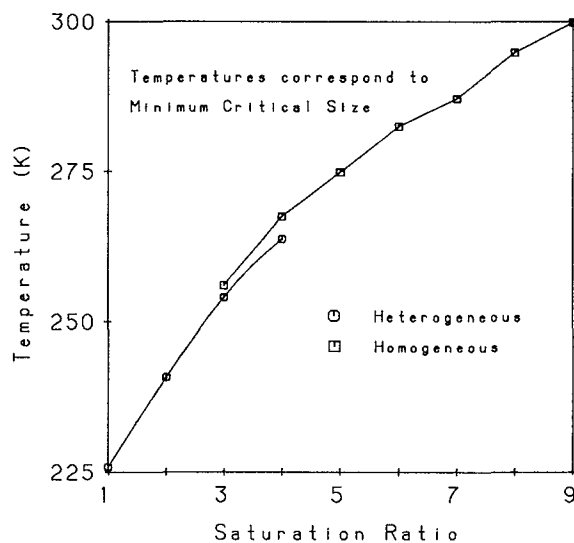

FIG. 15. Temperatures correspond to the minimum critical size of heterogeneous and homogeneous water clusters as a function of saturation ratio.
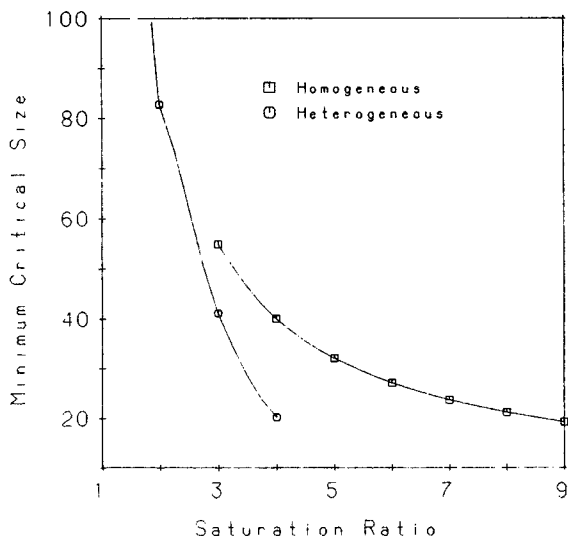
FIG. 16. Minimum critical size of heterogeneous and homogeneous water clusters as a function of saturation ratio.

water cluster and the surface. Furthermore, a simple analytic function was found to fit the binding energy vs cluster size relationship.

Encouragingly, the energies of formation and the critical sizes for heterogeneous clusters are well predicted to be smaller compared to the homogeneous case for given temperature and saturation ratio. Heterogeneous clusters exhibit a minimum at small cluster sizes, smaller than 12 water molecules. This is a property previously observed from an analytic theory[29] in the case of hydrated ion cluster nucleation.

At lower temperature for fixed saturation ratio, a linear relationship was observed between $\log(J)$ and $1/T$. Interestingly, at higher temperatures, deviations from linearity are observed. For saturation ratios around 2 and 3, maxima are observed in the $\log(J)$ vs $1/T$ curves, with maximum nucleation rates at temperature about 230 K. Unfortunately, to the best of our knowledge, there exist no measurements for comparison.

For a given saturation ratio, there is a temperature that corresponds to a minimum critical size. Furthermore, when the temperatures were plotted against saturation ratio, there is a region where the heterogeneous and homogeneous cases almost overlap. This suggests the occurrence of a minimum critical size, dependent on the water vapor concentration condition, not on the existence of the condensation nuclei.

It is of great interest in the future to have experimental verifications regarding various observations in the first-made study of heterogeneous nucleation based on a microphysical cluster approach.

ACKNOWLEDGMENTS

APPENDIX: MODIFIED AM1 METHOD

In order to computationally treat water nucleation onto silicon, we incorporated our HMNDO adaptation of the MNDO method into the current AM1 semiempirical program. The HMNDO adaptation, developed for water clusters alone, allows the water–water interactions to be properly handled, a feature lacking in the original AM1. The HMNDO method introduced a new parameter set for hydrogen (H) and oxygen (O) atoms, and this parameter set was position dependent in the sense that two parameter sets were used—one for intramolecular interactions and one for intermolecular interactions (Ref. 18).

The HMNDO technique is incorporated into AM1 for treating the water on the silicon system, i.e., systems containing hydrogen, oxygen, and silicon. It is important to note that practically all the hydrogen and oxygen parameters in HMNDO are different from those of AM1, including both the one center parameters and the two center terms. Any alteration in the one center parameters, i.e., the one center, one electron energies between s and s shells, and between p and p shells (USS and UPP), does not directly change the two center interactions, but through their contributions to the F matrix and thus to the eigenvalue problem, they will alter the wave functions (density matrix) and hence indirectly affect the two center interactions. Hence much care must be used in choosing the parameters and in their treatment in the computations. All interactions between water elements (H and O atoms) are calculated using the HMNDO parameter set. Interactions involving other atoms, i.e., silicon, are handled using AM1 parameters. For the hydrogen and oxygen one center, one electron energy terms (see Ref. 31), USS and UPP, weighted values between the HMNDO and AM1 values are used, with the weighting based on the environment in which the particular atom finds itself. The parameter values are more water-like (closer to those of HMNDO) when the atom is surrounded by mostly hydrogen and oxygen atoms; they are weighted towards the AM1 values when the atom is mostly surrounded by silicons.

Subroutines are added to the modified AM1 program which (1) store the electronic interaction energies for Si–H and Si–O from AM1; and for H–H, O–O, and O–H from HMNDO for a range of interatomic distances; and (2) determine a multiplicative "scale" factor for the USS and UPP of each water element (H or O). Then we use this scale factor in the main AM1 program. Whenever they appear, USS and UPP are multiplied by the scale factor scale defined below. For example, for a given atom W (either H or O) in the system, we define an environment function

$$\text{env}(W) = \frac{\sum_{W'} E_{\text{HMNDO},W,W'}(r_{W,W'})}{\sum_s E_{\text{AM1},W,S}(r_{W,S}) + \sum_{W'} E_{\text{HMNDO},W,W'}(r_{W,W'})},$$

(A1)

where $\sum_{W'}$ runs over all H's and O's, excluding atom W; and $\sum_s$ runs over all Si's. $E_{\text{HMNDO},W,W'}(r_{W,W'})$ denotes the total energy (electronic and nuclear) for the two atom W–W' cluster, calculated using the HMNDO parametri-

zation, separated by distance $r_{W,W'}$; $E_{AM1,W,S}(r_{W,S})$ denotes the total energy for the two atom (W–Si cluster, calculated using the AM1 parametrization, separated by distance $r_{W,S}$. Env(W) tends to unity when atom W is surrounded by H's and O's; it tends to zero when it is surrounded mostly by Si's. Note that env(W) depends clearly on the cluster's geometry. We determine the scale factor as

$$\text{scalef}(i,W) = 1 + \left(\frac{\zeta_{i,W,HMNDO}}{\zeta_{i,W,AM1}} - 1 \right) \text{env}(W). \quad (A2)$$

$\zeta_{i,W,HMNDO}$ is the corresponding HMNDO value for USS for UPP of atom W, and $\zeta_{i,W,AM1}$ is the corresponding AM1 value. Then in the main AM1 program, we include this scale factor in every appearance of USS and UPP. The scale factor is adjusted as the geometry changes, if geometry optimization is envoked.

[1] Report on the technical workshop, *The Future of Laboratory Research and Facilities for Cloud Physics and Chemistry*, Boulder, Colorado, March 1985.

[2] H. R. Byers, *Elements of Cloud Physics* (University of Chicago, Chicago, 1965), pp. 109–118.

[3] J. B. Mason, *The Physics of Clouds* (Oxford University, London, 1971), pp. 122–152.

[4] H. R. Pruppacher and J. D. Klett, *Microphysics of Clouds and Precipitation* (Reidel, Boston, 1978), pp. 225–281.

[5] (a) P. V. Hobbs, *Ice Physics* (Clarendon, Oxford, 1974), pp. 472–523; (b) *Clouds: their Formation, Optical Properties and Effects*, edited by P. V. Hobbs and A. Deepalk (Academic, New York, 1986); pp. 1–14 and 93–186.

[6] G. M. Hidy and J. R. Brock, *Aerosol Physics and Chemistry* (Pergamon, New York, 1970), Vol. 1, pp. 258–295.

[7] S. K. Friedlander, *Smoke, Dust, and Haze: Fundamentals of Aerosol Behavior* (Wiley, New York, 1977), pp. 235–261.

[8] J. H. Seinfeld, *Air Pollution: Physical and Chemical Fundamentals* (McGraw–Hill, New York, 1975), pp. 198–203.

[9] J. R. Smith, *Topics in Current Physics 19: Theory of Chemisorption* (Springer, New York, 1980).

[10] F. O. Goodman and H. Y. Wachman, *Dynamics of Gas–Surface Scattering* (Academic, New York, 1976).

[11] G. Benedek and U. Valbusa, *Springer Series in Chemical Physics 21: Dynamics of Gas–Surface Interaction* (Springer, New York, 1982).

[12] V. Ponec, Z. Knor, and S. Cerny, *Adsorption on Solids* (CRC, Boca Raton, FL, 1974).

[13] A. W. Adamson, *Physical Chemistry of Surfaces* (Wiley, New York, 1982), pp. 492–594.

[14] R. Eefay, I. Progogine, and A. Bellmans, *Surface Tension and Adsorption* (Wiley, New York, 1951).

[15] B. Lewis and J. C. Anderson, *Nucleation and Growth on Thin Films* (Academic, New York, 1978).

[16] A. Yoshimori and M. Tsukada, *Dynamical Processes and Ordering on Solid Surfaces* (Springer, New York, 1985).

[17] S. H. Suck Salk and C. K. Lutrus, *Lecture Notes in Physics*, edited by P. Wagner and G. Vali (Springer, New York, 1988), Vol. 309, p. 496.

[18] S. H. Suck Salk and C. K. Lutrus, J. Chem. Phys. **87**, 636 (1987); S. H. Suck Salk, T. S. Chen, D. E. Hagen, and C. K. Lutrus, Theor. Chim. Acta **70**, 3 (1986).

[19] S. H. Suck Salk and C. K. Lutrus, NATO ASI Ser. B **158**, 305 (1987).

[20] S. H. Suck Salk and C. K. Lutrus, Phys. Rev. A **42**, 6151 (1990).

[21] S. H. Suck Salk, C. K. Lutrus, and D. E. Hagen, J. Atmos. Sci. **45**, 2979 (1988).

[22] S. Tomoda and K. Kimura, Chem. Phys. Lett. **102**, 560 (1983).

[23] W. Thiel, Theor. Chim. Acta **48**, 357 (1978); M. Gordon, D. Tallman, C. Monroe, M. Steinbach, and J. Ambrust, J. Am. Chem. Soc. **97**, 1326 (1975); T. Zielenski, D. Breen, and R. Rein, *ibid.* **100**, 6266 (1978); G. Klopman, P. Andreozzi, A. Hoffinger, O. Kibuchi, and M. Dewar, *ibid.* **100**, 6268 (1978).

[24] K. Kimura, S. Katzumata, Y. Achiba, T. Yamazaki, and S. Iwata, *Handbook of Photoelectron Spectra of Fundamental Organic Molecules* (Halsted, New York, 1981).

[25] S. Tomoda, Y. Achiba, and K. Kimura, Chem. Phys. Lett. **87**, 197 (1982).

[26] A. Yencha, H. Kubota, T. Fukuyma, T. Kondow, and K. Kuuchitsu, J. Electron. Spectrosc. **23**, 431 (1981).

[27] D. Eisenberg and W. Kauzmann, *The Structure and Properties of Water* (Oxford University, London, 1969).

[28] L. A. Curtiss and J. A. Pople, J. Mol. Spectrosc. **55**, 1 (1975).

[29] S. H. Suck, T. S. Chen, R. W. Emmons, D. E. Hagen, and J. L. Kassner, Jr., Heterogeneous Atmos. Chem. Geophys. Monogr. Ser. **26**, 28 (1982).

[30] F. F. Abraham, *Homogeneous Nucleation Theory* (Academic, New York, 1974).

[31] M. J. S. Dewar and W. Thiel, J. Am. Chem. Soc. **99**, 4899 (1977).

[32] M. J. S. Dewar, E. G. Zoebisch, E. F. Healy, and J. J. P. Stewart, J. Am. Chem. Soc. **107**, 3902 (1985); M. J. S. Dewar and C. Jie, Organometallics **6**, 1486 (1987).

[33] S. H. Suck Salk, T. Oshiro, C. K. Lutrus, D. E. Hagen, and G. L. Loper, J. Korean Phys. Soc. **24**, 11 (1991).

[34] T. Oshiro, C. K. Lutrus, D. E. Hagen, and S. H. Suck Salk, Solid State Commun. (in press).

[35] C. K. Lutrus, T. Oshiro, D. E. Hagen, and S. H. Suck Salk, Phys. Rev. B (in press); A. Redondo, W. A. Goddard III, C. A. Swarts, and T. C. McGill, J. Vac. Sci. Technol. **19**, 498 (1981); A. Redondo, W. A. Goddard III, and T. C. McGill, *ibid.* **21**, 649 (1982); Surf. Sci. **132**, 49 (1983).

[36] U. Hofer, P. Morgen, W. Wurth, and E. Umbach, Phys. Rev. B **40**, 1130 (1989).

[37] M. Nishijima, K. Edamoto, Y. Kubota, and M. Onchi, J. Chem. Phys. **84**, 6458 (1986).

[38] H. Ibach and D. L. Mills, *Electron Energy Loss Spectroscopy and Surface Vibrations* (Academic, New York, 1982).

[39] H. Ibach, H. Wagner, and D. Bruchmann, Solid State Commun. **42**, 457 (1982).

[40] *Smithsonian Meteorological Table*, edited by R. J. List (Smithsonian Institution, Washington, D. C., 1971), p. 350.